

Experimental investigation of fretting wear in Ti-6Al-4V dovetail assemblies under resonant vibration

Xiyuan Zhang[1,2], Dasheng Wei[1,2] & Shun Yang[1,2]

[1]School of Energy and Power Engineering, Beihang University, Beijing 100191, China
[2]Jiangxi Research Institute, Beihang University, Nanchang 330096, China

Abstract

Dovetail assemblies in aeroengines are subjected to complex fatigue loading during service. The fretting wear behavior of Ti-6Al-4V dovetail assemblies under resonant vibration was investigated using fan blades manufactured with real geometry and a newly developed vibration test platform. The effects of clamping level, excitation load, and loading cycles on the resonance response of the blade and the evolution of surface wear on the dovetail tenon were systematically analyzed. Furthermore, the surface fretting wear induced by vibration loading was compared with that observed under low cycle fatigue conditions, highlighting the distinctive wear mechanisms and damage morphologies associated with resonant vibration. Finally, the dovetail tenon surface was treated using a mechanical shot peening process, and the effectiveness of shot peening in enhancing the fretting wear resistance of the dovetail joint was comprehensively evaluated through comparative analyses.

Keywords: Ti-6Al-4V fan, Dovetail assembly, Resonant vibration, Fretting wear, Shot penning.

1. Introduction

Dovetail assemblies are widely used in aeroengine fan blades because of their excellent load transfer capability and structural reliability [1,2]. As illustrated in Fig. 1, the fatigue loads experienced during service can be broadly divided into two categories: (1) low cycle fatigue caused by variations in rotational speed during takeoff and landing cycles, and (2) high cycle fatigue induced by complex vibratory loads during flight, such as aerodynamic excitation and engine order resonance. Both fatigue modes can significantly affect the reliability of dovetail assemblies, but their damage mechanisms are markedly different. Extensive studies [3] have investigated low cycle fretting fatigue associated with case (1). In contrast, the fretting fatigue and surface wear behavior of dovetail assemblies under resonant vibration conditions, corresponding to case (2), still require further experimental investigation and mechanistic analysis.

Fretting is a typical nonlinear contact phenomenon characterized by small amplitude relative motion between contacting surfaces subjected to normal and cyclic tangential loads [4]. The contact state continuously evolves among stick, partial slip, and gross slip regimes during cyclic loading, resulting in complex nonlinear behavior in friction, contact stiffness, and energy dissipation, which ultimately governs fretting wear and fretting fatigue damage [5,6]. Previous studies have shown that fretting behavior is strongly influenced by factors such as contact pressure, temperature, wear evolution, and relative slip amplitude [7,8].

For dovetail assemblies, extensive investigations have focused on low cycle fretting fatigue associated with radial tensile loading, as illustrated in Case (1) of Fig. 1. Experimental and numerical studies have revealed the effects of stress concentration, contact conditions, and surface strengthening treatments on fretting fatigue performance and life prediction [9,10]. However, compared with low cycle fretting fatigue, vibration induced fretting damage remains much less understood. This is mainly because vibration testing of blade structures is considerably more challenging. Existing vibration fatigue studies are generally concentrated on overall dynamic characteristics or fatigue damage in blade midspan regions, while the fretting behavior of dovetail joints has received relatively limited attention [11-12]. In addition, many experimental configurations

employ simplified boundary conditions or artificially constrained fixtures, making it difficult to accurately reproduce the actual contact characteristics of engineering dovetail assemblies.

In addition to vibration induced fretting wear, surface strengthening technologies have attracted increasing attention as effective approaches for improving the durability of dovetail assemblies. Among them, shot peening has been widely applied in aeroengine components due to its ability to introduce a gradient hardened layer and beneficial compressive residual stresses near the surface. Previous studies have demonstrated that shot peening can effectively suppress crack initiation and retard fatigue crack propagation under conventional fatigue and low cycle fretting fatigue conditions [13,14]. Moreover, the refined near surface microstructure and enhanced surface hardness produced by shot peening may alter the contact stress distribution, reduce local plastic deformation, and improve resistance to fretting wear. However, most existing investigations have focused on fatigue under tensile loading conditions [15], while the influence of shot peening on fretting wear evolution and contact damage behavior under resonant vibration conditions remains largely unexplored.

In this study, Ti-6Al-4V fan blades were manufactured with real structural geometry, and a newly developed vibration testing platform was employed to investigate the surface contact wear behavior under vibratory conditions. The effects of clamping level, excitation load amplitude, and cycle number on blade resonance characteristics and dovetail tenon wear evolution were systematically examined. In addition, vibration induced fretting wear was further compared with that generated under low cycle fatigue loading to clarify the characteristic wear features and damage mechanisms under resonant vibration. The dovetail tenon surface was then strengthened by mechanical shot peening, and its contribution to improving the anti-fretting wear performance of the dovetail joint was assessed through comparative experiments.

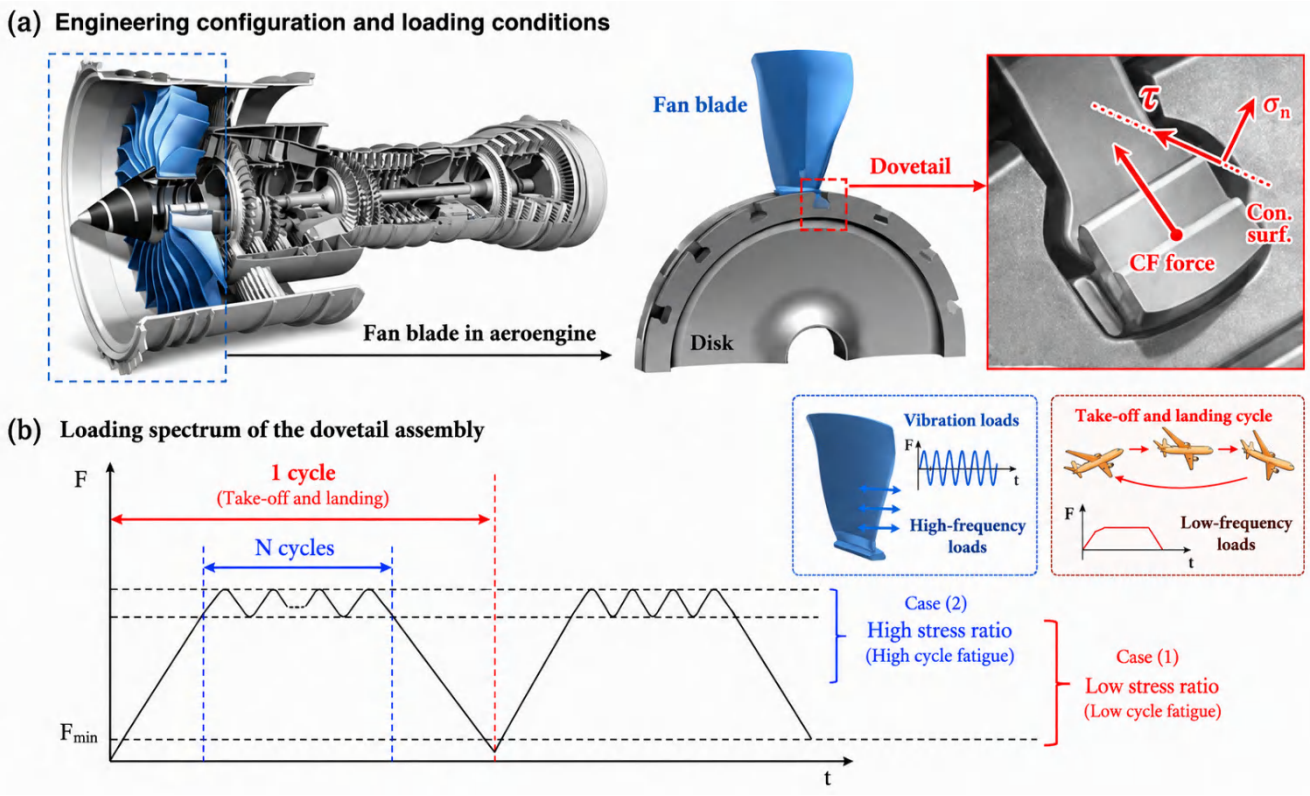


Figure 1 –Fretting fatigue issues in aeroengine fan blade dovetail assemblies. (a) Engineering configuration and representative loading conditions. (b) Loading spectrum, consisting of low cycle fatigue dominated by radial tensile loading and high cycle fatigue dominated by vibratory loading.

2. Testing procedure

2.1 Materials

TC4 possesses specific material properties, including an elastic modulus of 109 GPa, a Poisson's ratio of 0.34, a density of 4440 kg/m3, a yield strength of 880 MPa and an ultimate tensile strength of 938 MPa at room temperature. The chemical composition of the material is provided in Table 1.

The shot peening process was performed at an injection angle of 90° and a standoff distance of 350 mm, with the nozzle moving horizontally back and forth at a constant speed of 800 mm/min. The shot peening intensity was 0.15 mmA, as determined from the arc height of an A type Almen strip, and was controlled by the nozzle pressure, peening duration, and average shot diameter. S110 steel shots with a diameter of 0.3 mm were used, with an air pressure of 0.15 MPa and a mass flow rate of 10 kg/min.

Figs. 2(a) and (b) present the surface microscopic morphology of Ti-64 specimens before and after shot peening, respectively, while Fig. 3(d) provides measurements of the surface roughness Ra and Rz of TC4 specimens before and after shot peening treatment. Fig. 2(c) illustrate the 2D and 3D morphology of the specimen surface after shot peening at various electron microscope magnifications (i.e., 5x, and 20x). At 20x magnification, numerous small craters from the impact of shots on the specimen surface are evident, indicating significant plastic deformation post-shot peening. Fig. 2(e) compares the surface hardness of TC4 before and after shot peening. This increase in surface hardness hinders crack initiation and reduces frictional damage between the specimen and indenter.

Table 1 – Chemical composition of the Ti-6Al-4V alloy (wt.%).

Al	V	Fe	Si	C	N	H	O	Ti
5.5–6.8	3.5–4.5	0.30	0.15	0.10	0.05	0.01	0.20	Balance

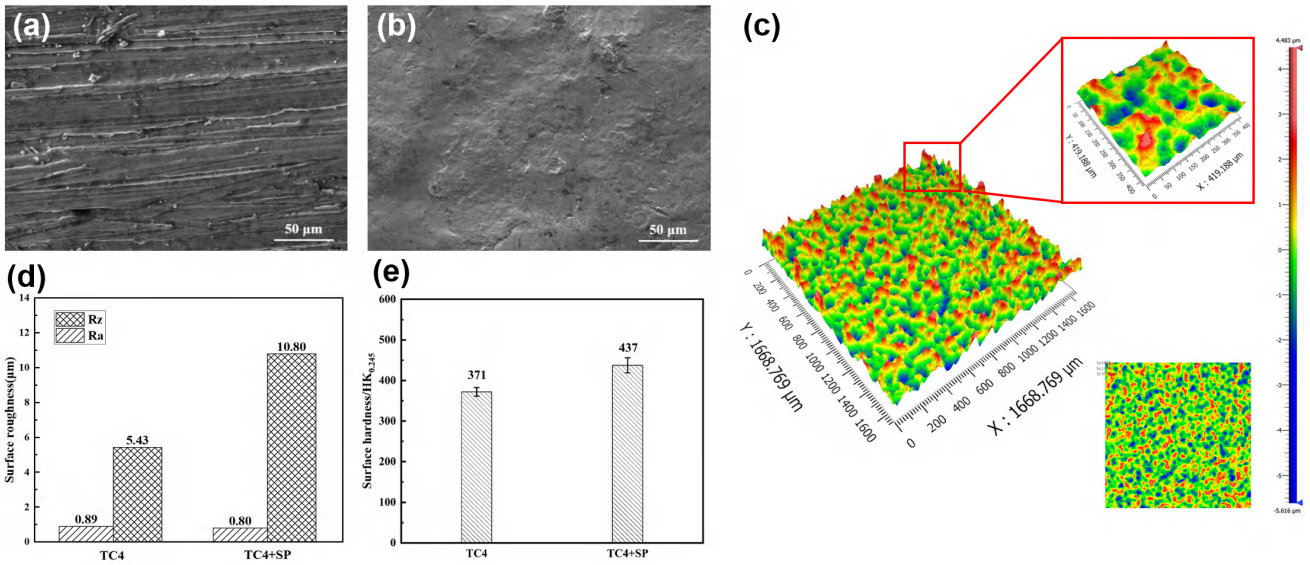


Figure 2 –Mechanical properties of Ti-6Al-4V. (a) Macroscopic surface morphology of the untreated specimen. (b) Macroscopic surface morphology after shot peening. (c) 3D surface morphology after shot peening. (d) Comparison of surface roughness. (e) Comparison of surface hardness.

2.2 Test platform

Based on a representative aeroengine fan blade configuration, three forged Ti-6Al-4V fan blades were designed and manufactured for the vibration fretting experiments. To enhance the vibration response under dynamic excitation and promote relative motion in the dovetail contact region, the blade aspect ratio was appropriately increased. The assembled test rig and its corresponding UG model are shown in Fig. 3.

The fixture frame was integrally machined from high strength 40Cr steel and rigidly bolted to the base. A replaceable Ti-6Al-4V groove liner was embedded in the mortise contact region to reproduce the actual dovetail contact conditions. This modular design allows only the blade and groove liner to be replaced after each test, ensuring an unworn contact interface for subsequent experiments.

The loading system consisted of two FPY-201 hydraulic jacks and a CP-180 manual hydraulic pump. The jacks were symmetrically positioned beneath the mortise and provided an upward load to simulate the centrifugal force experienced by the blade during service. Copper pads were inserted between the jacks and the dovetail tenon to improve load uniformity through local plastic deformation. In addition, transverse preload was applied through two M24 bolts installed on both sides of the

fixture frame. The preload direction formed an angle of 30° with the y-axis, consistent with the loading orientation in actual blade–disk assemblies. By adjusting the combination of jack force and bolt preload, the contact stress state of the dovetail interface under different rotational speeds could be reproduced. Self-locking washers were employed on all bolted connections to prevent loosening during long term vibration tests.

The excitation system utilized an ESD-100 permanent magnet modal exciter (Dongling Vibration Co., Ltd.), capable of generating sinusoidal excitation forces up to 1000 N within a frequency range of 5–6000 Hz. The system included a dedicated controller, power amplifier, acceleration sensors, and a threaded excitation rod. The rod was connected to the blade through a reserved hole and secured using two nuts with a rubber pad inserted between them to avoid local stress concentration.

The proposed platform enables simultaneous investigation of blade vibration characteristics and fretting wear behavior of dovetail assemblies. By varying the clamping force and excitation amplitude, the influences of loading conditions on resonance response, contact state evolution, and fretting wear behavior can be systematically evaluated.

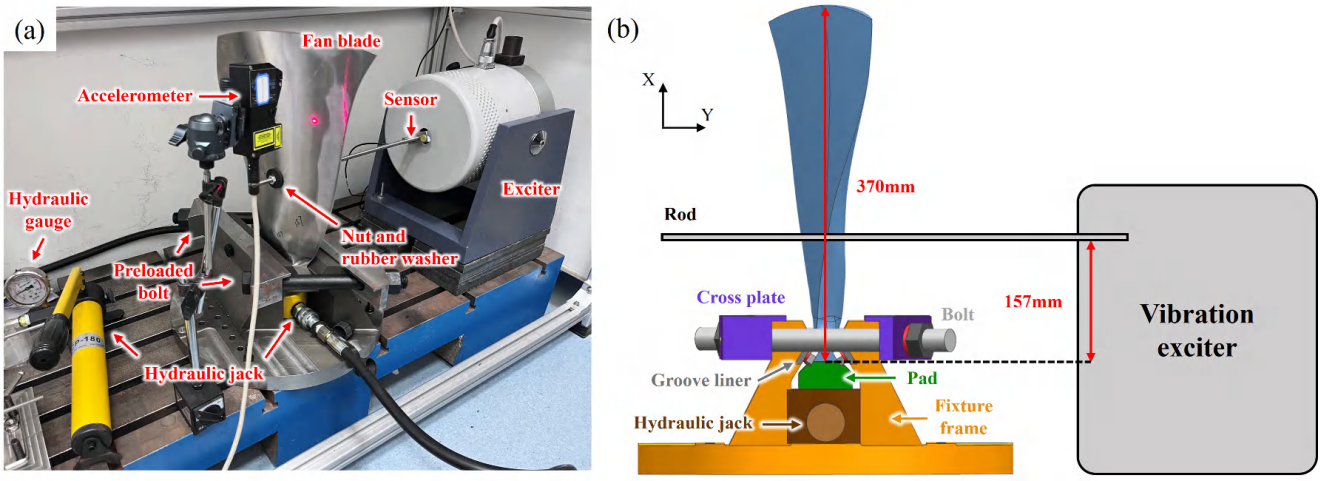


Figure 3 –Complete test platform: (a) assembled setup; (b) schematic of the overall structure.

2.3 Loading scheme

Two types of experiments were conducted in this study: vibration response (VR) tests of the fan blade and vibration fatigue (VF) tests of the fan blade dovetail assembly. In both tests, the clamping condition of the dovetail assembly was controlled by adjusting the jack force, while the excitation level was varied by changing the input vibration load. This design enabled a systematic evaluation of the effects of boundary constraints and excitation amplitude on the vibration response and damage evolution of the dovetail joint.

For the VR tests, four jack force levels were applied to each hydraulic jack, namely 10, 20, 40, and 60 kN, representing different clamping conditions. Meanwhile, six excitation levels were used, corresponding to acceleration amplitudes of 0.5, 1.0, 1.5, 2.0, 2.5, and 3.0 g, where 1 g = 9.8 m/s². The detailed test matrix is summarized in Table 2, covering groups VR-01 to VR-15.

Table 2 – Loading conditions and experimental scheme.

Test No.	Jack force (kN)	Preload torque (N·m)	Loads(g)	Frequency(Hz)	Cycles($\times 10^7$)
VR-01	20	80	1	110~150 (sweep)	-
VR-02			2		
VR-03			3		
VR-04			0.5		
VR-05			1.5		
VR-06			2.5		
VR-08	20	80	2	110~150 (sweep)	-
VR-09	60				
VR-10	10				

VR-11	10	80	1	110~150 (sweep)	-
VR-12			0.5		
VR-13			2.5		
VR-14			3		
VR-15			1.5		
VF-01	40	80	2	128	1
VF-02					2
VF-03					3
VF-04	40	80	3	128	1
VF-05					2
VF-06					3
SPVF-01	40	80	3	128	1

3. Results and discussion

3.1 Fan blade response under resonant vibration

The vibration response of the fan blade is strongly affected by the clamping condition of the dovetail assembly and the excitation amplitude. Figs. 4(a) and (b) present the frequency domain displacement responses under different excitation levels for jack forces of 40 kN and 10 kN, respectively. A clear resonance peak appears at approximately 130 Hz, while no other significant peaks are observed during the frequency sweep. This indicates that the dynamic response of the test system is mainly governed by the first vibration mode with limited influence from modal coupling or external disturbances.

For both jack force levels, increasing the excitation amplitude leads to a significant increase in the peak displacement response, accompanied by a slight decrease in the resonance frequency. This frequency reduction may be attributed to the enhanced nonlinear contact behavior at higher excitation levels, which slightly reduces the equivalent contact stiffness and results in minor structural softening. Under a jack force of 40 kN, the resonance frequency decreases from approximately 133 Hz to 128.1 Hz as the excitation increases from 0.5 g to 3 g, while the displacement amplitude increases from 0.285 mm to 0.972 mm. A similar trend is observed for the 10 kN case, where the displacement amplitude increases from 0.332 mm to 1.037 mm over the same excitation range, and the resonance frequency also decreases to 128.1 Hz.

Overall, the displacement response increases by more than three times as the excitation amplitude rises, whereas the resonance frequency decreases by only about 5 Hz. These results indicate that the fan blade vibration response is highly sensitive to excitation amplitude, while the variation in effective stiffness remains relatively limited. Therefore, the overall dynamic behavior of the system is still predominantly controlled by the first vibration mode.

Fig. 4(c) shows the frequency domain displacement responses under different jack forces, with the excitation load fixed at 2 g and the bolt preload torque maintained at 80 N·m. A single dominant resonance peak is observed, indicating that the response is still governed by the first mode. Variations in jack force only slightly affect the response: the non resonant displacement remains nearly unchanged, while minor differences appear near resonance. As the jack force increases, the peak displacement slightly decreases and the resonance frequency increases, which can be attributed to enhanced clamping and increased equivalent contact stiffness. As shown in Fig. 4(f), when the jack force increases from 10 kN to 60 kN, the resonance frequency rises from 129.2 Hz to 129.9 Hz, while the peak displacement decreases from 0.911 mm to 0.851 mm. Overall, jack force has a limited influence on the resonance characteristics compared with excitation amplitude.

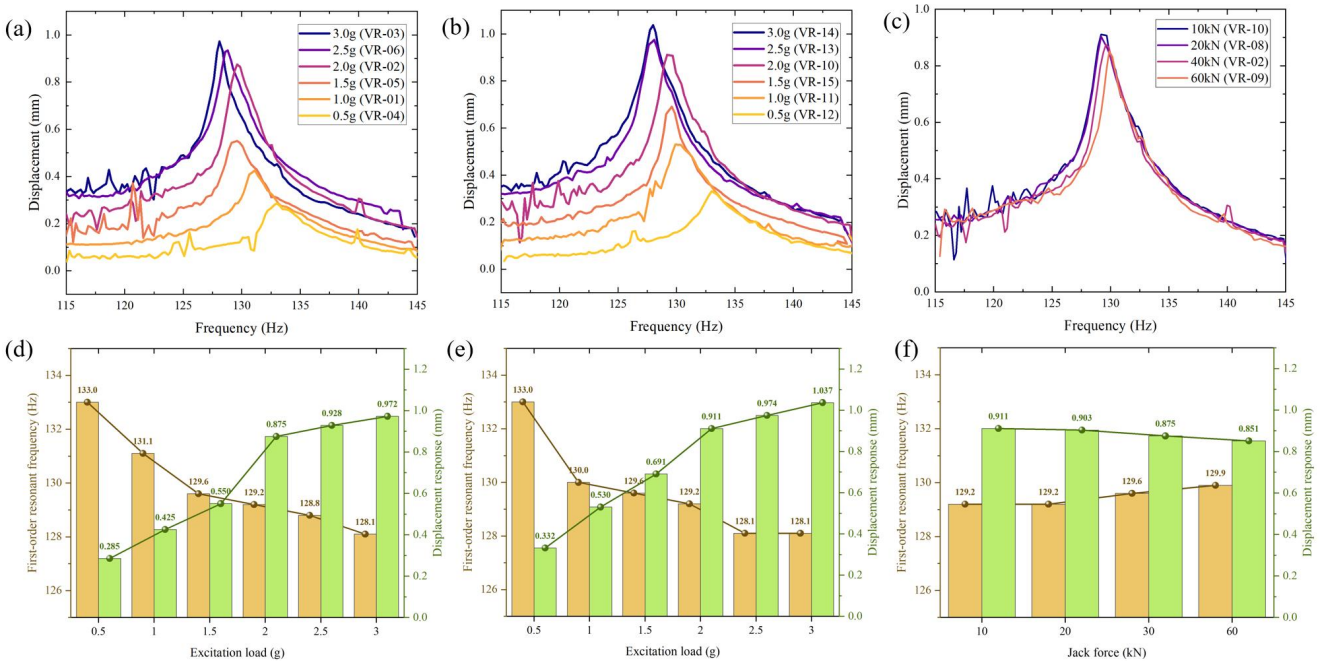


Figure 4 –Effect of excitation load on displacement response and resonance frequency. (a) Jack force of 40 kN and bolt preload torque of 80 N·m, corresponding to test groups VR-01–VR-06. (b) Jack force of 10 kN and bolt preload torque of 80 N·m, corresponding to test groups VR-10–VR-15. (c) Excitation load 2g and bolt preload torque 80 N·m, corresponding to test groups VR-02 and VR-08 to VR-10. (d,e,f) Resonance frequency and peak displacement of the corresponding test groups: (d) VR-01–VR-06, (e) VR-10–VR-15 and (f) VR-02 and VR-08 to VR-10.

3.2 Surface fretting wear of the fan blade tenon

The macroscopic wear morphology provides an overall view of wear distribution and its evolution with increasing cycle number, but it cannot accurately characterize the three dimensional surface profile. Therefore, a 3D white light interferometer was employed to further examine the severely worn regions within the contact zone. Owing to the limited measurement window of the instrument, representative areas were selected for detailed observation. The wear behavior is primarily governed by the relative slip and contact stress distribution between the dovetail tenon and groove, both of which are most pronounced near the contact zone edges.

Fig. 5 presents the microscopic surface morphology at the contact edge of specimen VF-02. The surface outside the contact zone remains largely intact and preserves the characteristic texture of the forged Ti-6Al-4V alloy. In contrast, severe wear is observed within the contact zone. Distinct wear grooves aligned with the dominant fretting slip direction are evident, together with local ploughing features produced by repeated material extrusion and removal. These observations indicate sustained fretting action, resulting in progressive plastic deformation and cumulative wear damage at the contact interface.

The 3D surface morphologies of regions 1 and 2 for specimens VF01 to VF06 at different cycle numbers are shown in Fig. 6. In the contour maps, red indicates higher elevations, and blue represents lower areas. Within the contact zone, wear-induced pits are randomly distributed, elongated along the u-axis (tangential direction of the surface), with significantly reduced height. Detached debris remains localized along pit edges, forming small piles, and accumulates extensively near the contact-zone boundary. Under cyclic loading, repeated compaction at the edges produces a distinct debris ridge along the contact boundary. Overall, the 3D morphologies reveal the evolution of wear from isolated pits to band-shaped grooves, illustrating continuous material loss within the contact zone and the extrusion and accumulation of material along boundaries. This process closely correlates with relative slip amplitude and local contact stress variations under fretting conditions.

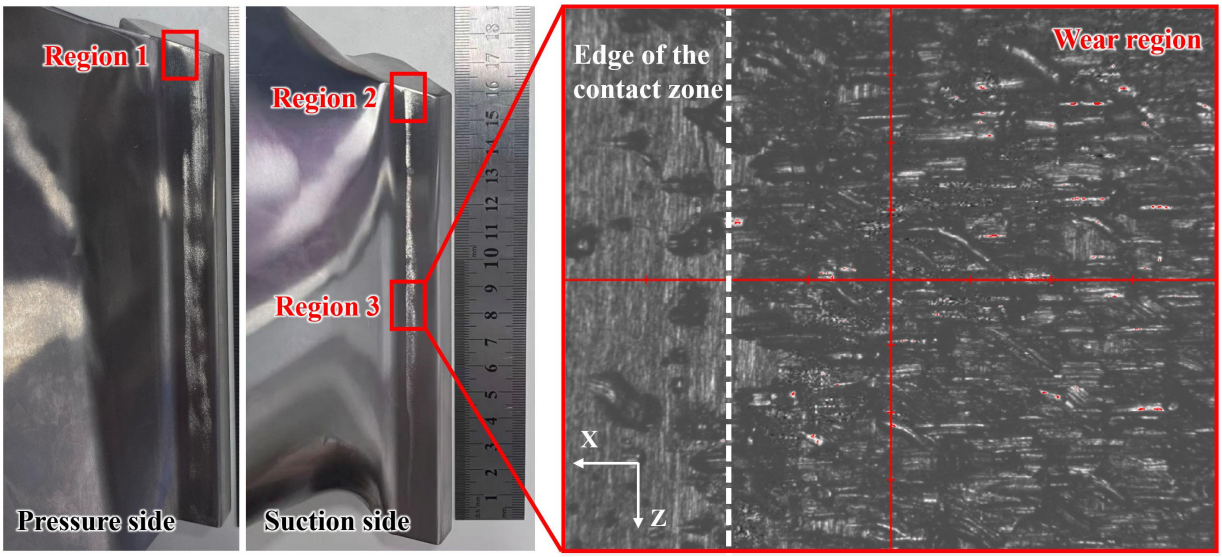


Figure 5 – Macroscopic wear morphology at the contact zone edge.

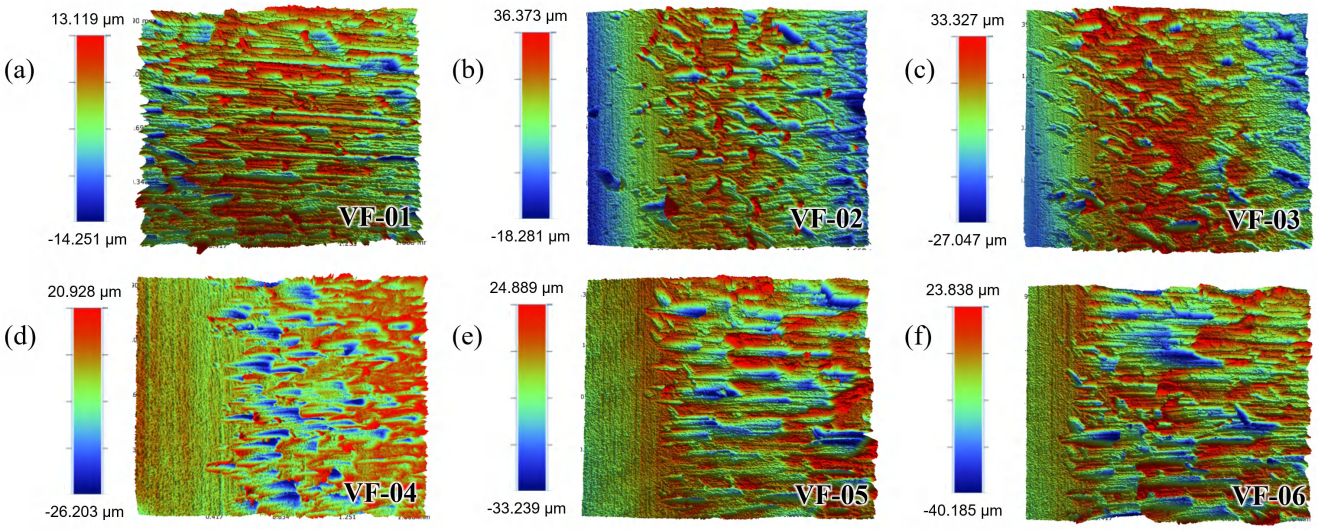


Figure 6 – 3D surface wear morphology of the tenon at the contact edge. (a)~(f): VF-01~VF-06.

To quantify the wear distribution along the relative sliding direction, the heights of all measured points at the same u-axis coordinate were arithmetically averaged, as shown in Fig. 19. This treatment reduces the influence of randomly distributed pits and provides a clearer representation of the height variation near the contact-zone edges. The averaged profiles show a consistent wear evolution at different cycle stages. With increasing cycle number, the average height within the contact zone gradually decreases, indicating progressive plastic deformation and material removal under long-term fretting. Meanwhile, the height peaks at the contact edges become more pronounced, suggesting the migration, compaction, and accumulation of wear debris under cyclic tangential loading, which eventually forms localized debris ridges. Overall, region 2 exhibits more severe wear than region 1, indicating that the contact edge on the suction side is more susceptible to wear damage under first-order bending resonance.

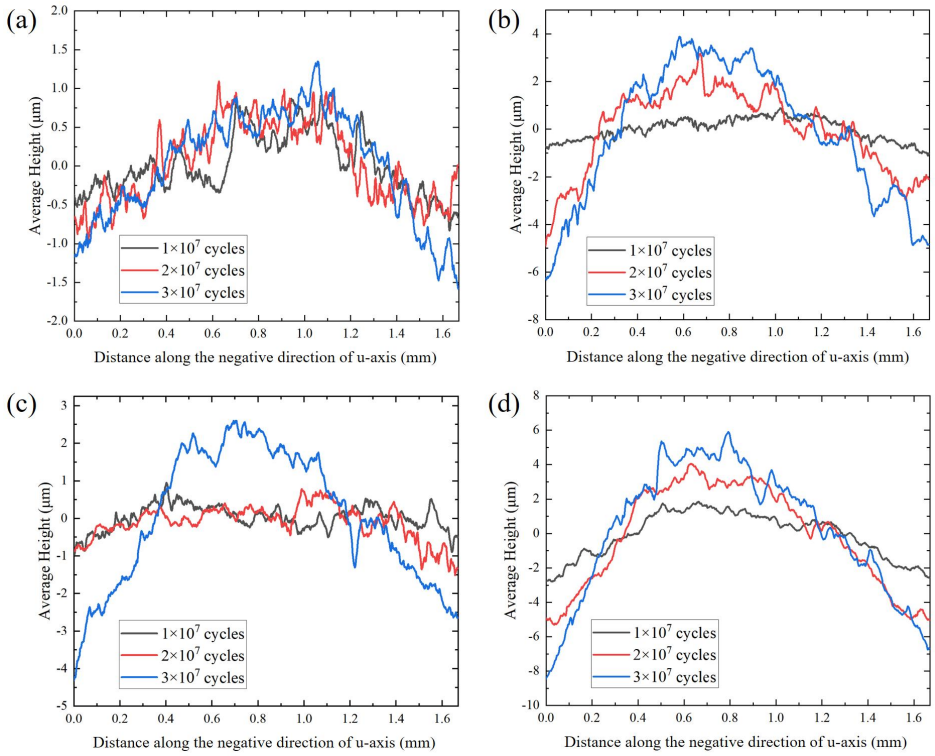


Figure 7 –Average height along the u-direction of the tenon wear surface at the contact zone edge. (a, b) VF-01 to VF-03 for Region Nos.: (a) Region 1, (b) Region 2. (c, d) VF-04 to VF-06 for region Nos.: (b) Region 1, (f) Region 2.

3.3 Comparison of fretting wear features under low cycle fatigue and vibration

To better illustrate the characteristics of vibration-induced fretting wear, Fig. 8 compares the surface damage produced under conventional low cycle fretting fatigue and resonant vibration conditions. Fig. 8(a) show a bridge-pad/flat specimen and a dovetail joint specimen, respectively, with the corresponding results reproduced from Refs. [10] and [16]. In all cases, the contacting components were fabricated from Ti-6Al-4V. The vibration-induced fretting wear obtained in the present study is presented in Fig. 8(c).

Fretting wear generally leads to material removal within the slip zone and wear debris accumulation near the contact boundaries. Consequently, the contact interface is often divided into sticking and slipping regions, which can be identified from both 3D surface topographies and mean height profiles. As shown in Fig. 8 (a1), the bridge-pad specimen exhibits a single wear pit accompanied by debris accumulation at the contact edges, resulting in a typical U-shape wear morphology that corresponds to a gross-slip condition. In contrast, the dovetail joint under low cycle fatigue loading exhibits multiple sticking regions and localized slip zones, producing a characteristic W-shape morphology with two distinct wear grooves, as confirmed by both the surface topography and mean height profile. The extent of the slip zone is mainly controlled by the contact pressure and cyclic load amplitude. Higher cyclic loads or lower stress ratios tend to promote relative sliding, whereas increased contact pressure suppresses slip and reduces the width of the slip zone.

A markedly different wear pattern is observed under resonant vibration conditions. As shown in Figs. 8(b1) and (c1), vibration-induced fretting generates a substantially wider slip zone, together with deeper and more numerous local wear pits. Unlike low cycle fatigue loading, which produces a stable and nearly unidirectional relative slip path, resonant vibration subjects the contact interface to high-frequency oscillations and continuously varying normal and tangential contact conditions. The resulting multidirectional relative motion increases frictional energy dissipation and promotes more extensive sliding across the contact interface. Simultaneously, repeated high-frequency crushing and shearing of surface asperities accelerate local material removal, leading to the formation of dense wear pits and debris clusters.

As a result, vibration-induced fretting wear exhibits a hybrid morphology. The 3D surface topography retains local W-shape features associated with multiple wear pits and debris accumulation, whereas the mean height profile resembles a U-shape distribution, with wear depth increasing continuously from the contact edges toward the center of the slip zone. This mixed wear pattern differs fundamentally from the classical U-shape and W-shape morphologies typically observed under low cycle fretting fatigue, highlighting the distinct wear mechanism associated with resonant vibration conditions.

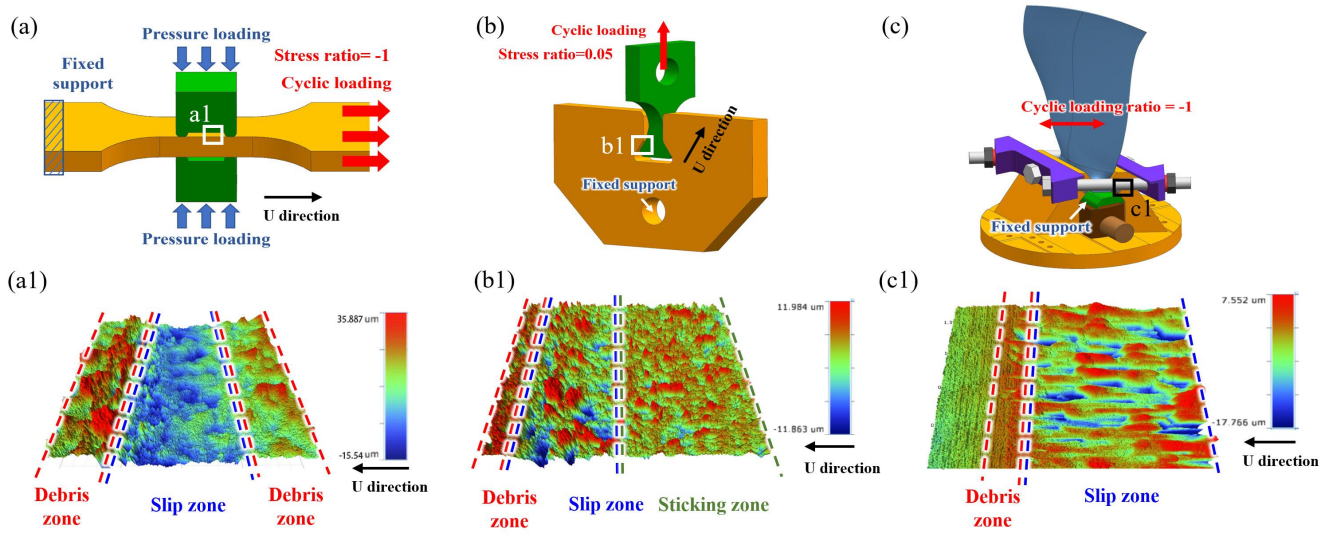


Figure 8 –. Typical fretting fatigue specimens and the corresponding 3D surface wear topography maps. (a) Bridge-type pad–plate fretting specimen. (b) Dovetail joints under low cycle fretting fatigue. (c) Dovetail joints under vibration-induced fretting fatigue.

3.4 Estimate of fretting wear

Fig. 9 compares the three-dimensional surface morphologies of the shot-peened and untreated specimens in Regions 1–3 after 1×10^7 loading cycles. Under the same loading conditions, the shot-peened specimens exhibit significantly better surface integrity. The wear depth within the contact zone is substantially reduced, while the size and density of wear pits are noticeably lower. In addition, the continuous groove-like wear features observed in the untreated specimens are markedly alleviated. Although wear debris accumulation can still be observed near the contact edges, the height of the debris ridges is considerably lower than that of the untreated specimens, indicating that shot peening effectively suppresses surface material removal, debris migration, and wear accumulation.

This improvement can be primarily attributed to the gradient strengthened layer and compressive residual stress field introduced by the shot peening process. On the one hand, work hardening increases the hardness and yield strength of the near-surface material, making it less susceptible to cumulative plastic deformation during fretting contact and thereby reducing the formation of wear pits and grooves. On the other hand, the compressive residual stress reduces the local tensile stress level at the contact surface and suppresses the initiation and propagation of microcracks, resulting in a lower wear debris generation rate and slower damage evolution. Furthermore, the strengthened surface layer provides enhanced support for surface asperities, improving the resistance of the contact interface to shear deformation and material spallation, thereby mitigating material removal during fretting.

To further quantify the wear severity, the average surface height along the u-direction within the investigated regions was calculated, as shown in Fig. 10. The averaged height profiles indicate that shot peening significantly reduces both the debris accumulation peaks at the contact-zone edges and the wear valley depths within the contact zone. Consequently, the overall wear amplitude is substantially lower than that of the untreated specimens. This effect is particularly evident in the regions exhibiting the most severe wear, where the height variation becomes noticeably smoother after shot peening. Quantitative analysis shows that the wear amplitude in Regions 1, 2, and 3

decreases by 12.0%, 34.2%, and 6.7%, respectively, after shot peening treatment. Among the three regions, Region 2 exhibits the most pronounced improvement, indicating that shot peening is especially effective in mitigating severe fretting damage in areas subjected to higher local contact stresses and relative slip amplitudes.

Overall, shot peening significantly enhances the fretting wear resistance of the dovetail joint contact interface, transforming the wear process from rapid accumulation to a more gradual evolution. It can therefore be expected that, under longer service cycles, the shot-peened specimens will continue to exhibit lower wear rates and better surface integrity, thereby delaying the progression of contact damage.

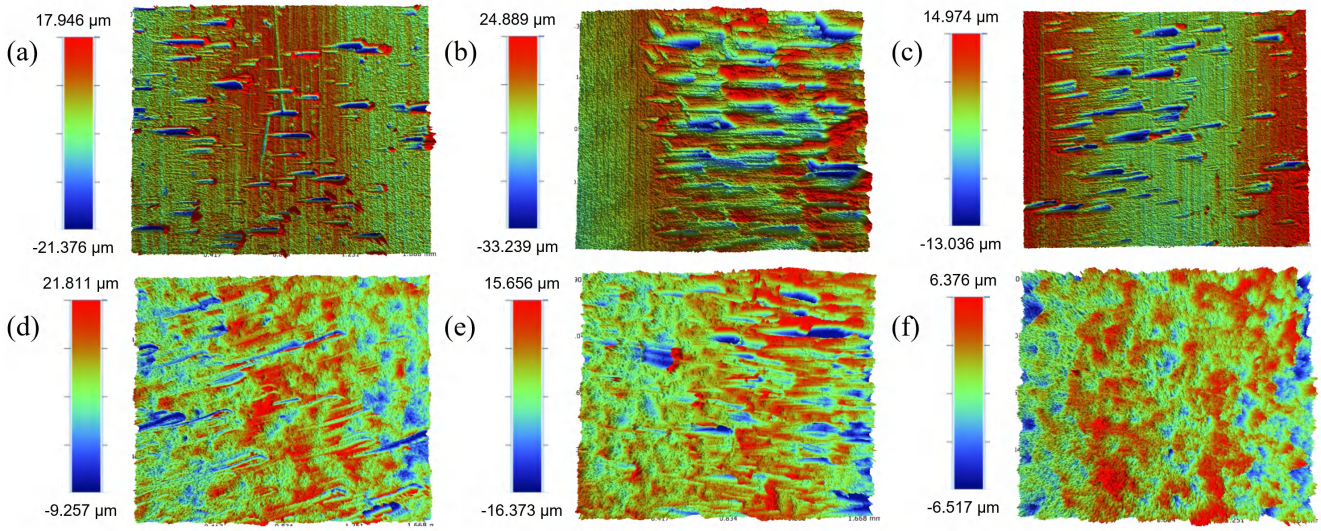


Figure 9 –. 3D surface wear morphology at the contact edge. (a)~(c): Un-peened tenon in Region 1, Region 2 and Region 3. (a)~(c): Shot-peened tenon in Region 1, Region 2 and Region 3.

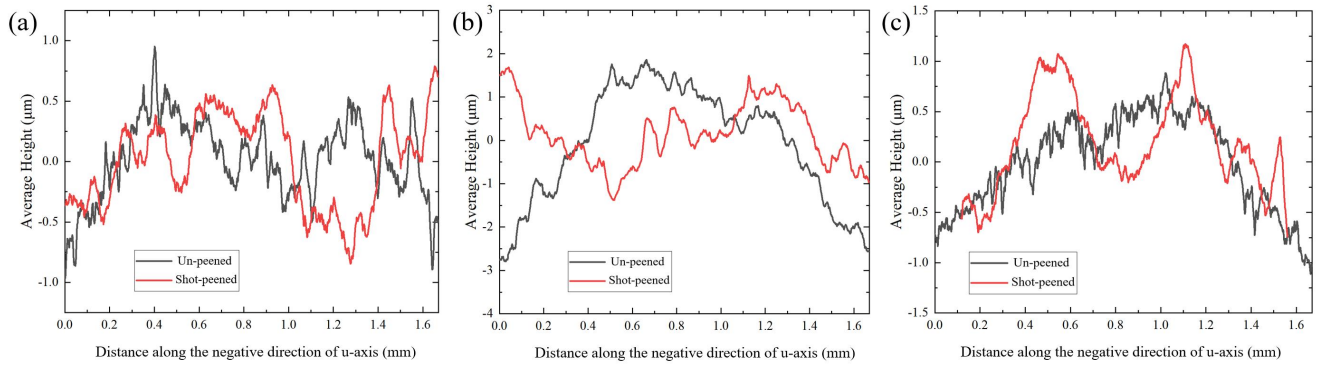


Figure 10 –. Average height along the u-direction of the shot-peened tenon wear surface at the contact zone edge. (a) Region 1 (a) Region 1, (b) Region 2. (c) Region 3.

4. Conclusions

A comprehensive experimental platform was established to investigate the vibration fretting response and fatigue behavior of fan blade dovetail joints. The main conclusions are as follows:

1) The displacement response is highly sensitive to both the excitation load and the clamping force of the dovetail assembly. Increasing the excitation from 0.5 g to 3 g causes the peak displacement to rise by 3.4 times, whereas increasing the dovetail clamping from 10 kN to 60 kN reduces the peak displacement by 7%.
2) Under first-bending-mode resonance, the suction side contact edge is more prone to wear. After 3×10^7 cycles, the maximum wear depth on the suction side exceeds that on the pressure side by 27%–70%, depending on excitation conditions. Despite severe fretting wear, no visible cracks were observed.
3) Compared with low cycle fretting, vibration-induced fretting wear exhibits a more pronounced W-shaped morphology. The worn surfaces contain numerous local pits and third-body debris, while

the average height profile resembles a U-shape, indicating a monotonic increase in wear depth from the contact edges toward the slip zone interior.

4) Shot peening significantly improves surface wear resistance. Compared with un-peened dovetail specimens, the average wear amplitude in different regions is reduced by 6%–35%, depending on local stress and fretting conditions.

5. Contact Author Email Address

Xiyuan Zhang: zhangxiyuan@buaa.edu.cn; Shun Yang: yangshun_academic@buaa.edu.cn

6. Copyright Statement

The authors confirm that they, and/or their company or organization, hold copyright on all of the original material included in this paper. The authors also confirm that they have obtained permission, from the copyright holder of any third party material included in this paper, to publish it as part of their paper. The authors confirm that they give permission, or have obtained permission from the copyright holder of this paper, for the publication and distribution of this paper as part of the ICAS proceedings or as individual off-prints from the proceedings.

References

[1] Glodek G, Gothivarekar S, Hooreweder B V, Talemi R. Investigating fretting fatigue response of additively manufactured Ti-6Al-4V in dovetail joint connections. Int J Fatigue 2025;199:109024.

[2] Hu C, Wei D, Wang Y, Jiang X. Introduction of fretting-contact-induced crack closure: Numerical simulation of crack initiation and growth path in disk/blade attachment. Chin J Aeronaut 2019;32(8):1923-1932.

[3] Mokhles M, Liu G, Shishavan B H, Dandekar T R, Barouni A, Birosca S. New insights on the deformation mechanism of fretting fatigue in Ti-6Al-4V. Acta Mater 2025;291:120998.

[4] Li X, Liu J, Liu J, Xu Y, Pan G, Shi Z. Dynamic modeling of a spline-shaft system including time-varying fretting friction. Int J Mech Sci 2025;294:110192.

[5] Glodek G, Van Hooreweder B, Talemi R. Interplay between subsurface defects and contact stress fields in the fretting fatigue response of additively manufactured Ti-6Al-4V. Theor Appl Fract Mech 2026;141:105278.

[6] Lefranc V, Baydoun S, Gandiolle C, Héripré E, Vallet M, Fouvry S, Aubin V. Heterogeneity in tribologically transformed structure (TTS) of Ti–6Al–4V under fretting. Wear 2023;522:204680.

[7] Razzak A, Wang S, Xue W, Gao S, Wu B, Duan D. Synergistic effects of load, displacement, and temperature on fretting wear behavior of Ti6Al4V alloy in self-mated contacts at elevated temperatures. Tribol Int 2026;214:111205.

[8] Wang Q, Chen X. Fretting fatigue crack initiation considering both wear and variable coefficient of friction. Tribol Int 2026;217:111632.

[9] Zhang X, Wei D, Yang S. Fretting fatigue in dovetail assembly and bridge-flat model: Verification of a life prediction model based on stress gradient. Int J Fatigue 2024;188:108500.

[10] Zhang X, Wei D, Ma M, Yang S. The effect of interfacial contact and damage gradient on fretting fatigue of Ti-6Al-4 V dovetail assembly using a multiaxial fatigue framework. Int J Fatigue 2025;199:109058.

[11] Zhang Z, Pan Y, Zhang Y, Li Q. Fatigue life and failure location prediction for notched structures subjected to multiaxial random vibration considering load correlation. Eng Fract Mech 2026;332:111736.

[12] Zhang Y, Zhang H, Ma H, Sun W, Du D, Xu K, Li H. Nonlinear vibration control of smart-composite-panels: Dynamic modeling and experimental testing. Int J Mech Sci 2026;311:111199.

[13] Zhang M, Zhu C, Zhao X, Huang Y, Wang S. The oil lubricated fretting wear behavior under different sliding displacements and frequencies of Ti6Al4V titanium alloy as affected by micro-shot peening. Wear. 2024, 548-549: 205386.

[14] Luo X., Dang N., Wang X. The effect of laser shock peening, shot peening and their combination on the microstructure and fatigue properties of Ti-6Al-4V titanium alloy. International Journal of Fatigue. 2021, 153:106465.

[15] Zhang X, Wei D, Liu X, Xiao J, Yang S. Effect of compressive residual stress and surface morphology introduced by shot peening on the improvement of fretting fatigue life of TC4. International Journal of Fatigue. 2025, 194:108835.

[16] Zhang X, Wei D, Liu X, Xiao J, Yang S. Effect of compressive residual stress and surface morphology introduced by shot peening on the improvement of fretting fatigue life of TC4. Int J Fatigue 2025;194.